http://dx.doi.org/10.5012/bkcs.2012.33.10.3285

Theoretical Study of Thiazole Adsorption on the (6,0) *zigzag* Single-Walled Boron Nitride Nanotube

Ali Varasteh Moradi,[*] Ali Ahmadi Peyghan,[†] Saeede Hashemian,[‡] and Mohammad T. Baei[§,*]

Department of Chemistry, Gorgan Branch, Islamic Azad University, Gorgan, Iran. [*]E-mail: avmoradi@yahoo.com
[†]Young Researchers Club, Islamic Azad University, Islamshahr Branch, Tehran, Iran
[‡]Department of Chemistry, Yazd Branch, Islamic Azad University, Yazd, Iran
[§]Department of Chemistry, Azadshahr Branch, Islamic Azad University, Azadshahr, Golestan, Iran. [*]E-mail: Baei52@yahoo.com
Received April 19, 2012, Accepted July 11, 2012

The interaction of thiazole drug with (6,0) *zigzag* single-walled boron nitride nanotube of finite length in gas and solvent phases was studied by means of density functional theory (DFT) calculations. In both phases, the binding energy is negative and presenting characterizes an exothermic process. Also, the binding energy in solvent phase is more than that the gas phase. Binding energy corresponding to adsorption of thiazole on the BNNT model in the gas and solvent phases was calculated to be −0.34 and −0.56 eV, and about 0.04 and 0.06 electrons is transferred from the thiazole to the nanotube in the phases. The significantly changes in binding energies and energy gap values by the thiazole adsorption, shows the high sensitivity of the electronic properties of BNNT towards the adsorption of the thiazole molecule. Frontier molecular orbital theory (FMO) and structural analyses show that the low energy level of LUMO, electron density, and length of the surrounding bonds of adsorbing atoms help to the thiazole adsorption on the nanotube. Decrease in global hardness, energy gap and ionization potential is due to the adsorption of the thiazole, and consequently, in the both phases, stability of the thiazole-attached (6,0) BNNT model is decreased and its reactivity increased. Presence of polar solvent increases the electron donor of the thiazole and the electrophilicity of the complex. This study may provide new insight to the development of functionalized boron nitride nanotubes as drug delivery systems for virtual applications.

Key Words : Boron nitride nanotubes, Drug delivery, Adsorption, Binding energy, Quantum molecular descriptors

Introduction

Nanomaterials have been employed to deliver biologically active cargo or therapeutic molecules to targeted cells into living systems for the purposes of disease diagnosis and therapy in a safe and efficient method.[1,2] The most important characteristics of drug delivery systems are including continuous regulation of drug levels within the therapeutic range, effective targeted delivery, reduction in the amount of drug essential, and a decrease in toxicity and side effects.[3,4]

Single-walled carbon nanotubes (SWCNTs), synthesized by Ijima in 1991,[5] can use as a highly efficient vehicle to transport a wide range of molecules across membranes into living cells.[6-8] However, one of the problems of nanotubes in drug delivery systems is their insolubility or poor solubility in common solvents.[9] Therefore to solve these problems, introduced various functional groups on the surface of the CNTs,[10,11] which enables chemical covalent bonding between the CNTs and foreign atoms or molecules.

The electronic properties of the CNTs depend on their diameter and chirality. Many investigations have been undertaken to investigate non-carbon-based nanotubes, which exhibit electronic properties independent of these parameters. Among such nanotubes, use of group III and V elements, which are the neighbors of C in the Periodic Table, has been an interesting subject of many studies, using materials such as boron nitride nanotubes (BNNTs).[12] BNNTs are inorganic analogs of CNTs and have good physical properties for a broad variety of applications; such nanotubes are always semiconductor with almost the same band gaps of 5.5 eV[13] and they are chemically, thermally stable,[14-17] and resistance to oxidation at high temperatures.[18]

However, the drug delivery properties of CNTs have been studied more often than those of BNNTs,[6-8] and further study of the drug delivery properties of BNNTs remains interesting. Therefore, it is important to understand the advantages and disadvantages of functionalizations of BNNTs for increase their biocompatibility, solubility, and further their application. Interaction of BNNTs to protein was studied by Zhi *et al*..[19] Their results showed that BNNTs may be particularly suitable for biological applications. Also, Ciofani and workers were used from folic acid as a targeting ligand to functionalize BNNTs against tumor cells.[20]

In this study, we used from (6,0) *zigzag* BNNT with thiazole (C3NH3S) biomolecule for potential applications to drug delivery and chemical modification of (6,0) *zigzag* BNNT model. Thiazole can further attached to other reactive groups or biological molecules such as drugs and used to deliver their cargos to cells and organs. Thiazole and its derivatives are very important in nature. The thiazole ring is

present in thiamine and plays a coenzyme for the oxidative decarboxylation of α-keto acids.[21] Its derivatives appear in vitamin B1and the skeleton of penicillin which is one of the first and still most important of the broad spectrum antibiotics. This heterocyclic compound is used in drug development for the treatment of inflammation,[22] hypertension,[23] bacterial[24] and HIV infections.[25] The determination of the structure of adsorbed thiazole on BNNT surfaces is also important for understanding its bonding and reactivity in catalysis and other surface phenomena and adsorption of thiazole on BNNTs may be able to yield changes in the interactions between the nanotube and foreign atoms or molecules.

Nuclear magnetic resonance (NMR) including isotropic and anisotropic chemical shielding (CS^I and CS^A) parameters[26] and nuclear quadrupole resonance (NQR)[27] spectroscopy are the best techniques to study the electronic structure properties of materials, could be well reproduced by density functional theory (DFT) calculations.[28,29] In previous cases, observed the efficiency of NMR and NQR parameters for the investigation of electronic properties of nanotubes.[28-31] Therefore, the objective of the present work is to study the quantum molecular descriptors[32,33] including electronic chemical potential (μ), global hardness (η), electrophilicity index (ω),[34] energy gap, global softness (S), electronegativity (χ), and ΔN,[35] and also investigation on binding energy, stability of the (6,0) *zigzag* BNNT model upon covalent functionalization with thiazole group, and the electronic structure properties of the thiazole -BNNT by performing density functional theory (DFT) calculations of the NMR and NQR parameters . Also, binding energy and stability of the (6,0) *zigzag* BNNT model in solvent phase are investigated to understand the role of solvent on electronic structure of the BNNT.

The electronic structure properties including bond lengths, bond angles, tip diameters, dipole moments, energies, energy gaps, NMR, and NQR parameters in the pristine and the thiazole -BNNT structures in gas and solvent (H_2O) phases were investigated by calculations of the chemical shift (CS) tensors at the sites of various ^{13}C, ^{11}B, and ^{15}N atoms and NQR calculations at the sites of ^{11}B and ^{14}N atoms.

Computational Methods

In the present work, the electronic structure properties and adsorption behavior of thiazole on the (6,0) *zigzag* BNNT was studied by means of density functional theory (DFT) calculations, in which the ends of the nanotube is saturated by hydrogen atoms. We investigated the influence of the attached thiazole on the properties of the (6,0) *zigzag* single-walled BNNT in gas and solvent (H_2O) phases as a drug and or functional group. The hydrogenated models of the pristine (6,0) *zigzag* BNNT and the thiazole-attached (6,0)BNNT model consisted of 60 atoms with formula of $B_{24}N_{24}H_{12}$ (pristine) and 68 atoms with formula of $B_{24}N_{25}H_{15}C_3S$. In the first step, all the atomic geometrical parameters of the structures were allowed to relax in the optimization at the DFT level of B3LYP exchange-functional and 6-31G* standard basis set in gas and solvent phases. The binding energy of the thiazole-attached (6,0)BNNT model was calculated as follows:

$$BE = E_{\text{Thiazole-BNNT}-} [E_{\text{BNNT}} + E_{\text{Thiazole}}] \quad (1)$$

Where $E_{\text{Thiazole-BNNT}}$ was obtained from optimization of the thiazole-attached (6,0) BNNT model, E_{BNNT} and E_{Thiazole} is the energy of the optimized BNNT and thiazole structures. The use of localized basis sets reliably reduces the amount of computational work required when using them with large vacuum regions in the unit cell. However, finiteness of the localized basis sets lead to basis set superposition errors (BSSE) as described by Tournus and Charlier in a study of benzene on CNTs.[36] To overcome this problem, BSSE has been estimated for the calculated structures by B3LYP in gas phase. This method was used to calculated, the binding energy (*BE*) of the thiazole-attached (6,0)BNNT model was calculated as follows:

$$BE = E_{\text{Thiazole-BNNT}-} [E_{\text{BNNT}} + E_{\text{Thiazole}}] + \delta_{\text{BSSE}} \quad (2)$$

Where δ_{BSSE} is the BSSE correction. A negative *BE* denotes exothermic process. Then, the CS tensors of the sites of various ^{11}B, ^{15}N, and ^{13}C atoms and NQR parameters of ^{11}B and ^{14}N were calculated for the optimized structures at the B3LYP /6-31G* level. It is noted that, when applying DFT methods, the B3LYP level usually gives more reliable results in comparison with experiments and is usually more convincing.[28,29] Moreover, in a previous study, it has been found that the NMR parameters calculated at the B3LYP and B3PW91 levels are in good agreement.[28] Therefore, all of the calculations were done at the B3LYP level. The calculated CS tensors in the principal axis system (PAS) with the order of $\sigma_{33} > \sigma_{22} > \sigma_{11}$ [37] were converted to measurable NMR parameters, *i.e.*, the isotropic CS (CS^I) and anisotropic CS (CS^A) parameters, using Eqs. (3) and (4)[28]; the NMR parameters of ^{11}B, ^{15}N, and ^{13}C atoms for the investigated (6,0) *zigzag* single-walled BPNT models are summarized in Table 4.

$$CS^I(\text{ppm}) = 1/3\ (\sigma_{11} + \sigma_{22} + \sigma_{33}) \quad (3)$$

$$CS^A(\text{ppm}) = \sigma_{33} - 1/2(\sigma_{11} + \sigma_{22}) \quad (4)$$

For NQR parameters, computational calculations do not directly detect return experimentally measurable NQR parameters, *i.e.*, the nuclear quadrupole coupling constant (C_Q), and asymmetry parameter (η_Q). Therefore, Eqs. (5) and (6) were used to calculate the EFG (electric field gradient) tensors to their proportional experimental parameters; C_Q is the interaction energy of the nuclear electric quadrupole moment (eQ) with the EFG tensors at the sites of quadrupole nuclei, but the asymmetry parameter (η_Q) is a quantity of the EFG tensors that describes the deviation from tubular symmetry at the sites of quadrupole nuclei. Nuclei with $I > 1/2$ (where I is the nuclear spin angular momentum) are active in NQR spectroscopy. The calculated EFG tensor eigenvalues in the principal axis system (PAS) with order

$|q_{zz}| > |q_{yy}| > |q_{xx}|$ were converted to measurable NQR parameters, *i.e.*, the nuclear quadrupole coupling constant (C_Q), and asymmetry parameter (η_Q), using Eqs. (5) and (6). The standard Q values [Q (^{11}B) = 40.59 and Q (^{14}N) =20.44 mb] reported by Pyykkö[38] are used in Eq. (5). The NQR parameters of ^{11}B and ^{14}N nucleus for the investigated (6,0) *zigzag* single-walled BPNT models are summarized in Table 5.

$$C_Q(\text{MHz}) = e^2 Q q_{zz} h^{-1} \quad (5)$$

$$\eta_Q = |(q_{xx} - q_{yy})/q_{zz}| \; 0 < \eta_Q < 1 \quad (6)$$

From the optimized (6,0) *zigzag* single-walled BPNT models, quantum molecular descriptors[32,33] including chemical potential (μ), global hardness (η), electrophilicity index (ω),[34] energy gap, global softness (S), and electronegativity (χ) were calculated as follows:

$$[\mu = -\chi = -(I + A)/2], [\eta = (I - A)/2], [\omega = \mu^2/2\eta],$$
$$\text{and } [S = 1/2\eta] \quad (7)$$

Where I ($-E_{HOMO}$) is the ionization potential and A ($-E_{LUMO}$) the electron affinity of the molecule. The electrophilicity index is a measure of electrophilic power of a molecule. The quantum molecular descriptors were compared for the pristine and the attached thiazole structure BNNT in gas and solvent phases. The global interaction between the thiazole drug molecule and the (6,0) BNNT can be showed by the parameter ΔN which determines the fractional number of electrons transferred from a system A to system B[35] and was calculated as follows:

$$\Delta N = (\mu_B - \mu_A)/2(\eta_A + \eta_B) \quad (8)$$

Where μ_A, μ_B and η_A, η_B are the chemical potential and chemical hardness of the systems A and B. A positive value of ΔN indicates that charge flows from B to A and the A act as an electron acceptor, while a negative value of ΔN indicates that charge flows from A to B and the A act as an electron donor. All the calculations were carried out by using the *Gaussian 03* suite of programs.[39]

Results and Discussion

Thiazole is as a precursor to many materials and useful compounds. For the adsorption of thiazole on the (6,0) BNNT, thiazole have three possible orientations toward the BNNT (*i.e.*, nitrogen, sulfur, and parallel orientations). We first study thiazole adsorption on the (6,0) BNNT with the orientations. After structural optimizations, it is found that thiazole adsorption with sulfur and parallel orientations on the BNNT are energetically unstable and are collapsed to the nitrogen orientation, which is energetically favorable. This trend is in agreement with the calculated molecular electrostatic potential surface (MEP) of the thiazole molecule. The MEP is the potential generated by the charge distribution of the molecule, which at an atomic site is defined as follows:

$$V(r) = \Sigma_A (Z_A/R_A\text{-}r) - \int \rho(r')\, dr'/|r'\text{-}r| \quad (9)$$

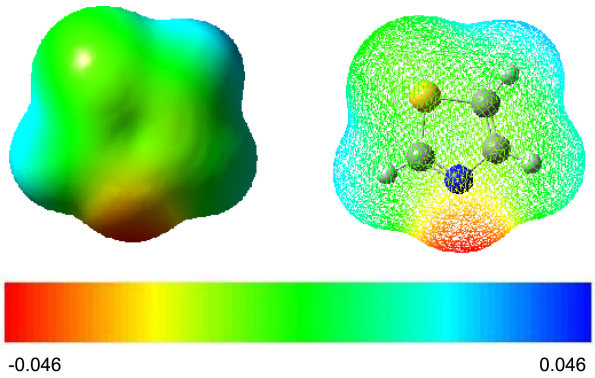

Figure 1. The molecular electrostatic potential surface of thiazole molecule.

Where Z_A is the charge on nucleus A, located at R_A. The V(r) depends on whether the effects of the nuclei or the electrons are dominant at any point. The MEP has been used to explore the chemical properties of several materials.[40,41]

The MEP surfaces of the single thiazole are shown in Figure 1. As shown by the MEP plot in Figure 1, in the thiazole molecule, just the nitrogen atom is negatively charged (red colors), while the carbon and sulfur atoms are neutral (green colors). Therefore, thiazole has one suitable orientation toward the BNNT (nitrogen orientation) and we limited our analysis to the interaction of thiazole with the nanotubes, nitrogen orientation which is the most common case (see Fig. 1).

Thiazole Adsorption on the (6,0) BNNT. The structural properties consisting of the B–N bond lengths, bond angles, tip diameters, dipole moments, energies, and energy gaps for the pristine and thiazole-attached (6,0) BNNT model in gas and solvent phases are summarized in Tables 1 and 2. All the atomic geometrical parameters of the structures were allowed to relax in the optimization at the DFT level of B3LYP exchange-functional and 6-31G* standard basis set in gas and solvent phases. Earlier studies revealed that the employed computational level of calculations could yield reliable results for the computational study of nanotubes in solvent phase.[42] In Figure 2, the atoms of the BNNT are numbered in order to describe the relevant structural parameters. The calculated results in Table 1 showed that the significant

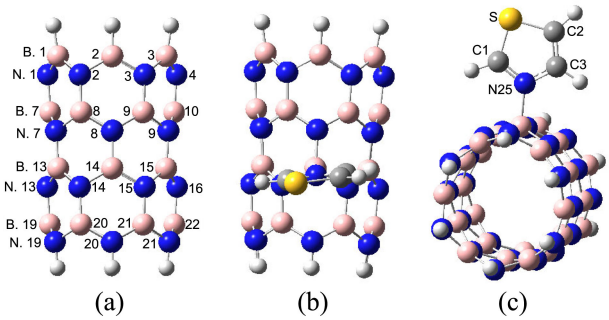

Figure 2. (a) Two-dimensional (2D) views of the pristine (6,0) *zigzag* BNNT (b) and (c) 2D and 3D views of the thiazole-attached (6,0)BNNT model.

Table 1. Structural properties of representative (6,0) *zigzag* BNNT models

Property	Thiazole-attached (6,0) BNNT		Pristine	Property	Thiazole-attached (6,0) BNNT		Pristine
bond length (Å)	Gas phase	Solvent Phase		bond length (Å)	Gas phase	Solvent Phase	
B1-6-H	1.19	1.19	1.19	N14-B20	1.44	1.45	1.45
N19-24-H	1.02	1.02	1.02	N15-B21	1.44	1.45	1.45
B1-N1	1.46	1.46	1.46	N16-B22	1.45	1.46	1.45
B1-N2	1.45	1.45	1.46	B19-N19	1.45	1.44	1.46
B2-N2	1.45	1.45	1.46	B20-N19	1.46	1.46	1.46
B2-N3	1.45	1.45	1.46	B20-N20	1.46	1.46	1.46
B3-N3	1.45	1.45	1.46	B21-N20	1.46	1.46	1.46
B3-N4	1.46	1.46	1.46	B21-N21	1.46	1.46	1.46
N1-B7	1.46	1.46	1.45	B22-N21	1.45	1.44	1.46
N2-B8	1.46	1.47	1.45	B14-N25	1.70	1.67	-
N3-B9	1.46	1.47	1.45	C1-N25	1.31	1.31	-
N4-B10	1.46	1.46	1.45	C1-S	1.72	1.71	-
B_7-N7	1.45	1.45	1.46	C2-S	1.74	1.74	-
B8-N7	1.46	1.46	1.46	C2-C3	1.36	1.36	-
B8-N8	1.45	1.44	1.46	C3-N25	1.38	1.38	-
B9-N8	1.45	1.44	1.46	Bond angles (°)			
B9-N9	1.46	1.46	1.46	N2-B2-N3	116.6	116.8	117.1
B10-N9	1.45	1.45	1.46	N7-B8-N8	119.4	119.7	118.2
N7-B13	1.45	1.46	1.45	N14-B14-N15	110.9	109.9	118.1
N8-B14	1.51	1.52	1.45	N20-B21-N21	121.3	121.0	122.2
N9-B15	1.45	1.46	1.45	B1-N2-B2	112.1	112.0	112.1
B13-N13	1.46	1.47	1.46	B7-N7-B8	111.0	111.1	110.2
B13-N14	1.44	1.44	1.46	B13-N14-B14	116.4	117.3	110.7
B14-N14	1.54	1.54	1.46	B20-N20-B21	108.5	108.7	111.2
B14-N15	1.53	1.54	1.46	N14-B14-N25	106.0	107.4	-
B15-N15	1.44	1.43	1.46	N25-C1-S	113.6	113.6	-
B15-N16	1.46	1.47	1.46	S-C2-C3	110.1	100.1	-
N13-B19	1.45	1.46	1.45	C2-C3-N25	114.0	113.9	-

changes of geometries including B-N bond lengths and the bond angles in the investigated (6,0) *zigzag* BNNT model in both phases is limited to atoms located in the immediate neighborhood of the thiazole, whereas those of other atoms remain almost unchanged. The change in bond lengths of B14-N14, B14-N15, and N8-B14 from 1.46 and 1.45 Å in pristine model to 1.54 and 1.52 Å in the thiazole-attached (6,0)BNNT models is associated to covalent attachment of thiazole functional group on the (6,0) BNNT sidewall (Table 1) leading to change in hybridization from sp^2 to sp^3 at the B-N bonds.

The calculated results in Table 2 show that the calculated energy value for the thiazole-attached (6,0) BNNT model in solvent phase is more than that gas phase. For evaluation the interaction of thiazole with the (6,0) *zigzag* BNNT model, the binding energy (*BE*) in the both phases are studied. In the thiazole-attached (6,0) BNNT model, the binding energy (*BE*) is negative, which characterizes a exothermic process. Also, the *BE* in solvent phase is more than that gas phase that show increase in thermodynamic stability of the thiazole-attached (6,0) BNNT model in solvent phase. Increase of thermodynamic stability of the complex in presence of H_2O solvent proposes the increasing of solubility of drugs by the thiazole-attached (6,0) BNNT model in solvent phase. The basis set superposition errors (*BSSE*) has been estimated for the calculated *BE* in gas phase by Eq. (2). In this method, the *BE* of the thiazole-attached (6,0)BNNT model is reduced (Table 2). Furthermore, in the investigated (6,0) *zigzag* BNNT models, it should be noted that B atoms

Table 2. Optimized properties of representative (6,0) *zigzag* BNNT models

Property	Thiazole-attached (6,0) BNNT		Pristine	Thiazole
	Gas phase	Solvent Phase		
E_T/keV	-67.7356	-67.7358	-52.2522	-15.4831
BE/eV	-0.34	-0.56	-	-
BE (δ_{BSSE})/eV	-0.13	-	-	-
Dipole moment/Debye	11.97	18.55	7.96	1.41
Diameter (B-tip)/Å	4.83	4.82	4.84	-
Diameter (N-tip)/Å	5.24	5.20	5.10	-
energy gap/eV	4.16	4.57	4.89	6.11

E_T = total energy, *BE* = binding energy

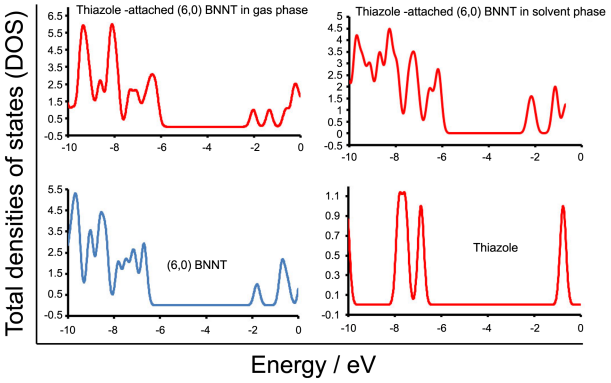

Figure 3. Total densities of states (DOS) for thiazole and different BNNT models.

relax in, while N atoms relax out, with respect to the nanotube surface. The dipole moments of the thiazole-attached (6,0)BNNT structure showed notable changes due to the thiazole adsorption with respect to the pristine model in gas and solvent phases. Also, the dipole moment for the model in solvent phase is more than that gas phase. It is important to note that the point charges are balanced in pristine the (6,0) *zigzag* BNNT model but these conditions are corrupted in the thiazole-attached (6,0)BNNT structure.

Electronic Properties of the (6,0) zigzag BNNT Complex.

Densities of States (DOS) of the Complex: To better understand the nature of interaction between thiazole with the (6,0) *zigzag* BNNT, we studied the influence of attached thiazole on the electronic properties of the (6,0) *zigzag* BNNT model in gas and solvent phases. The total densities of states (DOS) of these tubes are shown in Figure 3. As is evident from Figure 3, the calculated energy gap of the perfect (6,0) *zigzag* single-walled BNNT is 4.89 eV,[12] whereas the calculated energy gaps of the thiazole-attached (6,0) BNNT model are 4.16, 3.90 eV in gas and solvent phase. The DOS of these tubes show changes due to thiazole adsorption in the gaps regions of the TDOS plots. Therefore, in comparison with the pristine model, the adsorption of thiazole on the BNNT decreases the energy gap of the pristine BNNT, and increases their electrical conductance. Also, thiazole adsorption in the solvent phase has a stronger effect than the thiazole adsorption in the gas phase on the energy gap of the BNNT.

Molecular Orbital (MO). The highest occupied molecular orbital (HOMO) and lowest unoccupied molecular orbital (LUMO) for thiazole, the pristine, and the thiazole-attached (6,0) BNNT model in gas and solvent phase are plotted in Figure 4. For the pristine model, HOMO is localized on the nitrogen atoms of the (6,0) *zigzag* BNNT model and corresponds to the lone pair of electron on nitrogen atoms. In contrast, LUMO is uniformly distributed throughout the B-N bonds. For the thiazole-attached (6,0) BNNT model in gas phase, HOMO is localized on the more electronegative nitrogen atoms of the model, especially on the nitrogen atoms of vicinity of the thiazole, whereas LUMO highly centered on the thiazole ring and small amount distributed on the nitrogen atoms of vicinity of the

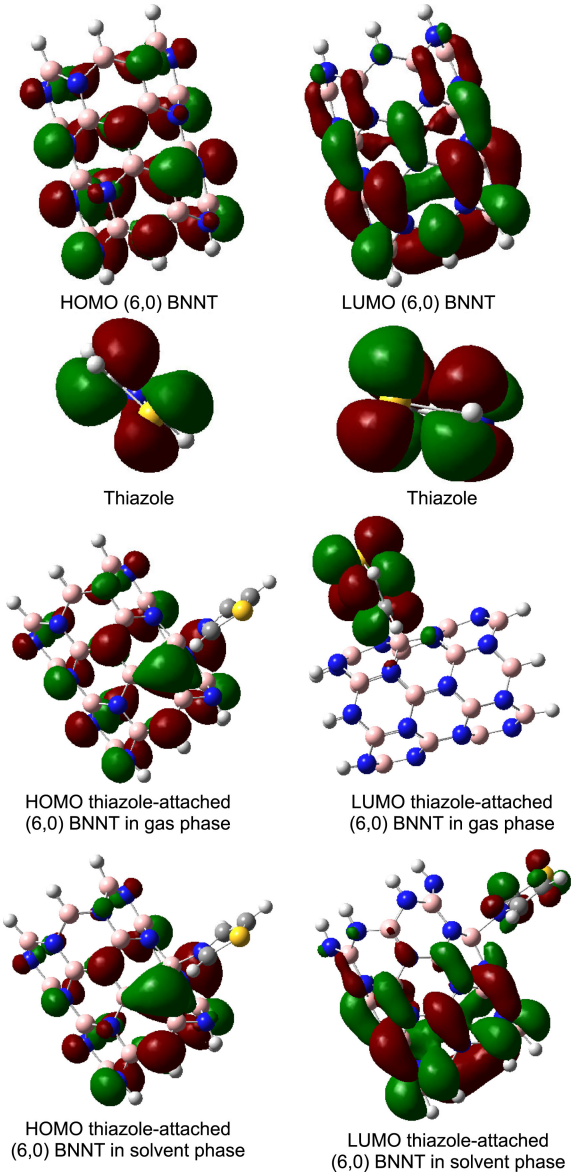

Figure 4. Orbital's of HOMO and LUMO for thiazole and different BNNT.

thiazole ring. The HOMO for the thiazole-attached (6,0) BNNT model in solvent phase is localized on the more electronegative nitrogen atoms of the model, especially on the nitrogen atoms of vicinity of the thiazole, whereas LUMO is distributed on the thiazole ring and the edge B-N bonds of the nanotube, which is basically due to unequal charge distribution along the edge B-N bonds (Fig. 4).

One of the most important factors in HOMO/LUMO interactions is the energy difference between HOMO of the thiazole molecule (nucleophile agent) and LUMO of the nanotube (electrophile agent). Our frontier molecular orbital theory (FMO) analysis indicate that HOMO energy of the thiazole molecule (nucleophile agent) is −6.86 eV, and that of LUMOs for the thiazole-attached (6,0) BNNT complex are −2.02 and −2.22 eV in gas and solvent phases (see Table 3), suggesting that the further value of *BE* for the complex in solvent phase (−0.56 eV) may come from its lower LUMO

energy level (−2.22 eV). Furthermore, it can be concluded that less negative *BE* value (−0.34 eV) for the complex in gas phase might be related to its higher LUMO energy level (−2.02 eV). An interesting conclusion that can be drawn from these investigations is that this factor can affect the values of *BEs*.

Quantum Molecular Descriptors. The quantum molecular descriptors for thiazole, the pristine, and thiazole-attached (6,0) BNNT models in gas and solvent phase are summarized in Table 3. We observe that in the thiazole-attached (6,0) BNNT model, the energy gap (E_{LUMO} - E_{HOMO}) decreases in the both solvent phases. This lowering of energy gap with functional group may be able to increase reactivity of the thiazole-attached (6,0) BNNT complex, and show charge transfer to takes place between the functional group and (6,0) BNNT sidewall. The global hardness and ionization potential of the thiazole-attached (6,0) BNNT model decreases with decrease in energy gaps of the model in the both phases. Decrease in global hardness, energy gap and ionization potential is due to the adsorption of thiazole, and consequently, the stability of the complex in the both phases is lowered and its reactivity increased. The value of hardness, softness, electerophilicity and chemical potential for the thiazole-attached (6,0) BNNT model is differing from the individual tube and thiazole molecule. In the presence of thiazole as a molecule interacting with BNNT, the capacity of the BNNT to attract electrons was diminished and the hardness of the thiazole-attached (6,0) BNNT model was decreased, which means decreased stability of the system. In addition, as the hardness of the BNNT is larger than the thiazole-attached (6,0) BNNT model, we can predict that the BNNT is relatively stable and thiazole adsorption process is dominant. These results are consistent

Table 3. Quantum molecular descriptors of representative (6,0) *zigzag* BNNT models

Property	Thiazole-attached (6,0) BNNT		Pristine	Thiazole
	Gas phase	Solvent Phase		
E_{HOMO}/eV	-6.18	-6.12	-6.68	-6.86
E_{LUMO}/eV	-2.02	-2.22	-1.79	-0.75
[E_{LUMO} - E_{HOMO}]/eV	4.16	3.90	4.89	6.11
[I = - E_{HOMO}]/eV	6.18	6.12	6.68	6.86
[A= - E_{LUMO}]/eV	2.02	2.22	1.79	0.75
[$\eta = (I - A)/2$]/eV	2.08	1.96	2.44	3.06
[μ = - (I + A)/2]/eV	-4.10	-4.17	-4.24	-3.80
[$S = 1/2\eta$]/eV^{-1}	0.24	0.26	0.20	0.16
[$\omega = \mu^2/2\eta$]/eV	4.04	4.46	3.68	2.36
ΔN	-0.04	-0.06	-	-

I = ionization potential, A = electron affinity, η = Global hardness, μ = Chemical potential, ω = electrophilicity

Table 4. NMR parameters/ppm of representative (6,0) *zigzag* BNNT models for sites of various ^{11}B, ^{15}N, and ^{13}C atoms

nucleus	Thiazole-attached (6,0) BNNT				Pristine		nucleus	Thiazole-attached (6,0) BNNT				Pristine	
	Gas phase		Solvent Phase					Gas phase		Solvent Phase			
	CS^I	CS^A	CS^I	CS^A	CS^I	CS^A		CS^I	CS^A	CS^I	CS^A	CS^I	CS^A
B1	76.6	52.1	77.0	51.2	76.0	52.8	N1	100.1	226.3	101.7	224.4	100.4	225.8
B2	76.8	52.2	77.4	51.4	76.0	52.8	N2	98.1	225.8	99.1	224.6	100.4	225.8
B3	76.6	52.3	77.1	51.4	76.0	52.8	N3	98.1	225.9	99.1	224.9	100.4	225.8
B4	76.2	52.5	76.5	51.9	76.0	52.8	N4	100.2	226.2	101.8	224.3	100.4	225.8
B5	76.1	52.6	76.5	52.0	76.0	52.8	N5	100.5	225.5	102.2	223.4	100.4	225.8
B6	76.2	52.5	76.6	51.9	76.0	52.8	N6	100.6	225.6	102.3	223.6	100.4	225.8
B7	79.4	38.5	79.3	38.4	79.2	38.6	N7	133.1	180.9	133.9	178.8	131.2	183.5
B8	80.2	37.8	80.4	37.2	79.2	38.6	N8	140.9	171.8	138.6	174.8	131.2	183.5
B9	80.1	38.3	80.4	37.8	79.2	38.6	N9	133.7	180.7	134.2	178.9	131.2	183.5
B10	79.3	38.5	79.3	38.4	79.2	38.6	N10	131.5	183.3	132.2	181.2	131.2	183.5
B11	78.9	39.0	78.8	38.9	79.2	38.6	N11	131.1	183.1	131.8	181.1	131.2	183.5
B12	79.0	39.0	78.9	38.9	79.2	38.6	N12	131.6	183.6	132.3	181.5	131.2	183.5
B13	79.9	34.8	80.0	34.1	78.6	36.4	N13	136.5	173.4	137.2	173.9	135.5	176.2
B14	104.7	4.4	106.8	3.9	78.6	36.4	N14	148.6	139.8	147.6	140.6	135.5	176.2
B15	80.2	34.6	80.2	34.0	78.6	36.4	N15	146.2	144.4	144.5	145.5	135.5	176.2
B16	78.5	36.5	78.3	36.3	78.6	36.4	N16	136.8	175.0	137.5	173.4	135.5	176.2
B17	78.1	36.8	77.9	36.7	78.6	36.4	N17	135.3	175.8	135.9	174.1	135.5	176.2
B18	78.5	36.5	78.3	36.3	78.6	36.4	N18	135.3	175.8	135.9	174.1	135.5	176.2
B19	81.4	39.6	80.5	40.0	81.3	40.1	N19	161.8	85.5	162.2	95.9	161.5	91.2
B20	81.2	40.3	80.7	40.9	81.3	40.1	N20	162.6	73.0	161.2	82.9	161.5	91.2
B21	81.6	39.6	81.0	40.0	81.3	40.1	N21	161.8	85.4	162.3	95.5	161.5	91.2
B22	81.5	39.7	80.6	40.0	81.3	40.1	N22	162.5	88.1	162.7	97.7	161.5	91.2
B23	80.8	40.7	80.0	41.0	81.3	40.1	N23	160.8	91.0	161.2	100.1	161.5	91.2
B24	80.9	40.6	80.0	41.0	81.3	40.1	N24	162.5	88.0	162.8	97.6	161.5	91.2
C1	37.7	139.9	35.3	146.4	-	-	N25	-25.4	304.6	-12.2	285.1	-	-
C2	69.7	118.2	66.2	126.3	-	-	S	281.1	167.5	271.6	189.3	-	-
C3	57.1	114.3	58.4	113.5	-	-							

with the results of the *BE* of thiazole-attached (6,0) BNNT model. The amount of charge transfer between the thiazole molecule and the (6,0) BNNT, as calculated using the ΔN method, is given in Table 3. A positive value of ΔN indicates that the thiazole act as an electron acceptor, while a negative value of ΔN indicates that the thiazole act as an electron donor. In the thiazole-attached (6,0) BNNT model, ΔN value is negative, indicating that thiazole molecule act as electron donor. The ΔN value of the complex in presence of H_2O solvent is more than that in gas phase. Therefore, presence of polar solvent increases the electron donor of the thiazole. The electrophilicity index is a measure of electrophilic power of a molecule. The electrophilicity of the complex in presence of H_2O solvent is much further from the electrophilicity of the complex in gas phase. Therefore, presence of polar solvent increases the electrophilicity of the complex.

NMR Parameters of the (6,0) zigzag BNNTs. The NMR parameters for the investigated (6,0) *zigzag* BNNTs models in gas and solvent phases is summarized in Table 4. In the pristine (6,0) *zigzag* BNNT, there are 24 B and 24 N atoms and the NMR parameters are separated into four layers: 1-6, 7-12, 13-18, and 19-24 (Table 4 and Fig. 1(a)). In the thiazole-attached (6,0) BNNT complex (Fig. 1(b)), the thiazole is directly bonded to B14atom, which results in a new B–N bond. Therefore the CS^I and CS^A values of the B14 atom that is directly bonded to the N25 atom of thiazole show the most significant changes due to direct effect of interaction of thiazole with the (6,0) *zigzag* BNNT in gas and solvent phases. The CS^I value of the B14 atom is increased, whereas the CS^A value of the atom is decreased very much. In comparison with the pristine model, the B14 atom is significantly influenced by the thiazole molecule. For the other B atoms of the model, the changes of the CS^I and CS^A values of the B atoms are almost negligible. For the N atoms of thiazole-attached (6,0) BNNT model, the CS^I and CS^A values of N8, N14, and N15 atoms, which are indirectly bonded to the B14 atom and are nearest neighbors of the B14 atom, show the most significant changes due to direct effect of thiazole interaction with the (6,0) *zigzag* BNNT in gas and solvent phases among the N atoms of the model, the CS^I value of the atoms are increased, whereas the CS^A value of the atoms are decreased. For the other N atoms of the model, the changes of the CS^I and CS^A values of the N atoms are almost negligible. These results are in agreement with the results of the quantum molecular descriptors and the *BE* of the thiazole-attached (6,0) BNNT model. Also, the calculated results presented in Table 4 indicate that the NMR parameters for the thiazole-attached (6,0) BNNT model are almost the same in the both phases.

NQR Parameters of the (6,0) zigzag Models. The NQR parameters at the sites of various ^{11}B and ^{14}N atoms for the optimized investigated (6,0) *zigzag* BNNT models are summarized in Table 5. There are 24 B and 24 N atoms in the considered (6,0) *zigzag* models, and the NQR parameters are separated into four layers based on the similarity of the calculated electric field gradient (EFG) tensors in each layer. The results in Table 5 show that the calculated NQR parameters are not similar for various nuclei, hence, the electrostatic environment of the BNNT is not equivalent throughout the lengths of the nanotube models. In Figures 1, the B1and N19 atoms shows the position of the first layer, B7 and N13 atoms shows the position of the second layer, the B13 and N7 atom shows the position of the third layer, and the B19 and N1 atoms shows the position t of the fourth layer in the considered *zigzag* models. The calculated results in Table 5 showed that there aren't significant difference in NQR parameters of the thiazole-attached (6,0) BNNT model with respect to the pristine (6,0) BNNT model except for B14 and N25 atoms that show significant changes in NQR parameters. These results are in agreement with the results of the NMR parameters and the structural properties the thiazole-attached (6,0) BNNT model. Because, the significant changes of geometries including B-N bond lengths and the bond angles in the thiazole-attached (6,0) BNNT model is limited to atoms located in the immediate neighborhood of the thiazole, whereas those of other atoms remain almost unchanged.

Table 5. The ^{11}B and ^{14}N NQR parameters

nucleus	Thiazole-attached (6,0) BNNT Gas phase		Pristine	
	C_Q/MHz	η_Q	C_Q/MHz	η_Q
B1	3.72	0.27	3.75	0.28
B7	3.00	0.07	3.00	0.09
B13	2.93	0.10	2.96	0.07
B19	2.78	0.12	2.80	0.10
B14	1.59	0.11	2.96	0.07
N1	0.94	0.45	0.97	0.45
N7	0.98	0.04	1.09	0.09
N13	1.12	0.12	1.18	0.07
N19	2.54	0.89	2.57	0.83
N25	2.18	0.34	-	-

Conclusions

We studied the adsorptions of thiazole as a drug and or functional group in gas and solvent (H_2O) phase. Also, we investigated the effects of thiazole adsorption on the the electronic structure properties, the quantum molecular descriptors, the NMR and NQR parameters of the thiazole-attached (6,0) BNNT model in gas and solvent phases by means of density functional theory (DFT) calculations. Also, binding energy and stability of the thiazole-attached (6,0) BNNT model in solvent phase are investigated to understand the role of solvent on electronic structure of the BNNT. In the thiazole-attached (6,0) BNNT model, the binding energy is negative and presenting characterizes a exothermic process. Also, the binding energy in solvent phase is more than that gas phase. Increase of thermodynamic stability of the complex in presence of H_2O solvent proposes the increasing of solubility of drugs by the thiazole-attached (6,0) BNNT model in solvent phase. The adsorption of thiazole on the

BNNT models decreases energy gap of the (6,0) BNNT, and increases its electrical conductance. The calculated results showed that the significant changes of geometries including B-N bond lengths, the bond angles, the NMR and NQR parameters in the investigated (6,0) *zigzag* BNNT models are limited to atoms located in the immediate neighborhood of the thiazole, whereas those of other atoms remain almost unchanged. The dipole moments of the thiazole-attached (6,0) BNNT structure showed notable changes due to the thiazzole adsorption with respect to the pristine model in the both phases and the values of dipole moment indicate that the reactivity of the complex in solvent phase is more than that in gas phase. Decrease in global hardness, energy gap and ionization potential because of functional group proposes the lowering of stability and increase in reactivity of the thiazole-attached (6,0) BNNT model in both phases. The ΔN value of the complex in solvent phase is more than that in gas phase and presence of polar solvent increases the electron donor of the thiazole. Presence of polar solvent increases the electron donor and the electrophilicity of the complex. In summary, our results show that thiazole molecule can be adsorbed on the surface of the BNNT with significant adsorption energies and charge transfer, which could show significant changes in the electrical conductivity of the BNNT.

Acknowledgments. This work was financially supported by Islamic Azad University, Gorgan Branch.

References

1. Leuschner, C.; Kumar, C. In *Nanofabrication Towards Biomedical Application*; Jormes, J., Leuschner, C., Eds.; Wiley-VCH: 2005; pp 289-326.
2. Ferrari, M. *Nature Rev.* **2005**, *5*, 161.
3. Bianco, A.; Kostarelos, K.; Partidos, C. D.; Prato, M. *Chem. Commun.* **2005**, *5*, 571.
4. Bianco, A.; Kostarelos, K.; Prato, M. *Biology* **2005**, *9*, 674.
5. Ijima, S. *Nature* **1991**, *354*, 56.
6. Prato, M.; Kostarelos, K.; Bianco, A. *Acc. Chem. Res.* **2008**, *41*, 60.
7. Kam, N. W. S.; Dai, H. *Physica Status Solidi B: Basic Solid State Phys.* **2006**, *243*, 3561.
8. Klumpp, C.; Kostarelos, K.; Prato, M.; Bianco, A. *Biochim. Biophys. Acta* **2006**, *1758*, 404.
9. Thess, A.; Lee, R.; Nikolaev, P.; Dai, H. J.; Petit, P.; Robert, J.; Xu, C. H.; Lee, Y. H.; Kim, S. G.; Rinzler, A. G.; Colbert, D. T.; Scuseria, G. E.; Tomanek, D.; Fischer, J. E.; Smalley, R. E. *Science* **1996**, *273*, 483.
10. Hirsch, A. *Angew Chem. Int. Ed. Engl.* **2002**, *41*, 1853.
11. Dyke, C. A.; Tour, J. M. *Chem. Eur. J.* **2004**, *10*, 812.
12. Baei, M. T.; Soltani, A.; Moradi, A. V.; Tazikeh, L. E. *Comput. Theoret. Chem.* **2011**, *970*, 30.
13. Blase, X.; Rubio, A.; Louie, S. G.; Cohen, M. L. *Euro. Phys. Lett.* **1994**, *28*, 335.
14. Rubio, A.; Corkill, J. L.; Cohen, M. L. *Phys. Rev. B* **1994**, *49*, 5081.
15. Loiseau, A.; Willaime, F.; Demoncy, N.; Hug, G.; Pascard, H. *Phys. Rev. Lett.* **1996**, *76*, 4737.
16. Bengu, E.; Marks, L. D. *Phys. Rev. Lett.* **2001**, *86*, 2385.
17. Nirmala, V.; Kolandaivel, P. *J. Mol. Struct. (Theochem)* **2007**, *817*, 137.
18. Solozhenko, V. L.; Lazarenko, A. G.; Petitet, J. P. *J. Phys. Chem. Solids* **2001**, *62*, 1331.
19. Zhi, C.; Bando, Y.; Tang, C. *J. Am. Chem. Soc.* **2005**, *127*, 17144.
20. Ciofani, G.; Raffa, V.; Menciassi, A.; Cuschieri, A. *Nanoscale Res. Lett.* **2009**, *4*(2), 113.
21. Breslow, R. *J. Am. Chem. Soc.* **1958**, *80*, 3719.
22. Haviv, F.; Ratajczyk, J. D.; DeNet, R. W.; Kerdesky, F. A.; Walters, R. L.; Schmidt, S. P.; Holms, J. H.; Young, P. R.; Carter, G. W. *J. Med. Chem.* **1988**, *31*, 1719.
23. Patt, W. C.; Hamilton, H. W.; Taylor, M. D.; Ryan, M. J.; Taylor, D. G., Jr.; Connolly, C. J. C.; Doherty, A. M.; Klutchko, S. R.; Sircar, I.; Steinbaugh, B. A.; Batley, B. L.; Painchaud, C. A.; Rapundalo, S. T.; Michniewicz, B. M.; Olson, S. C. J. *J. Med. Chem.* **1992**, *35*, 2562.
24. Tsuji, K.; Ishikawa, H. *Bioorg. Med. Chem. Lett.* **1994**, *4*, 1601.
25. Bell, F. W.; Cantrell, A. S.; Hoegberg, M.; Jaskunas, S. R.; Johansson, N. G.; Jordon, C. L.; Kinnick, M. D.; Lind, P.; Morin, J. M., Jr.; Noreen, R.; Oberg, B.; Palkowitz, J. A.; Parrish, C. A.; Pranc, P.; Sahlberg, C.; Ternansky, R. J.; Vasileff, R. T.; Vrang, L.; West, S. J.; Zhang, H.; Zhou, X.-X. *J. Med. Chem.* **1995**, *38*, 4929.
26. Bovey, F. A. *Nuclear Magnetic Resonance Spectroscopy*; Academic Press: San Diego, 1988.
27. Das, T. P.; Han, E. L. *Nuclear Quadrupole Resonance Spectroscopy*; Academic Press: New York, 1958.
28. Baei, M. T.; Sayyed Alang, S. Z.; Moradi, A. V.; Torabi, P. *J. Mol. Model* **2011**, doi: 10.1007/s00894-011-1130-4
29. Baei, M. T.; Moradi, A. V.; Torabi, P.; Moghimi, M. *Monatsh Chem.* **2011**, *142*, 783.
30. Baei, M. T.; Moradi, A. V.; Moghimi, M.; Torabi, P. *Comput. Theoret. Chem.* **2011**, *967*, 179.
31. Baei, M. T.; Moradi, A. V.; Torabi, P.; Moghimi, M. *Monatsh Chem.* **2011**, *142*, 1097.
32. Chattaraj, P. K.; Sarkar, U.; Roy, D. R. *Chem. Rev.* **2006**, *106*, 2065.
33. Hazarika, K. K.; Baruah, N. C.; Deka, R. C. *Struct. Chem.* **2009**, *20*, 1079.
34. Parr, R. G.; Szentpaly, L.; Liu, S. *J. Am. Chem. Soc.* **1999**, *121*, 1922.
35. Parr, R. G.; Pearson, R. G. *J. Am. Chem. Soc.* **1983**, *105*, 7512.
36. Tournus, F.; Charlier, J. C. *Phys. Rev. B* **2005**, *71*, 165421.
37. Drago, R. S. *Physical Methods for Chemists*, 2nd ed.; Saunders College Publishing: Florida, 1992.
38. Pyykkö, P. *Mol. Phys.* **2001**, *99*, 1617.
39. Frisch, M. J.; Trucks, G. W.; Schlegel, H. B.; Scuseria, G. E.; Robb, M. A.; Cheeseman, J. R.; Zakrzewski, V. G.; Montgomery, J. A., Jr.; Stratmann, R. E.; Burant, J. C.; Dapprich, S.; Millam, J. M.; Daniels, A. D.; Kudin, K. N.; Strain, M. C.; Farkas, O.; Tomasi, J.; Barone, V.; Cossi, M.; Cammi, R.; Mennucci, B.; Pomelli, C.; Adamo, C.; Clifford, S.; Ochterski, J.; Petersson, G. A.; Ayala, P. Y.; Cui, Q.; Morokuma, K.; Malick, D. K.; Rabuck, A. D.; Raghavachari, K.; Foresman, J. B.; Cioslowski, J.; Ortiz, J. V.; Baboul, A. G.; Stefanov, B. B.; Liu, G.; Liashenko, A.; Piskorz, P.; Komaromi, I.; Gomperts, R.; Martin, R. L.; Fox, D. J.; Keith, T.; Al-Laham, M. A.; Peng, C. Y.; Nanayakkara, A.; Gonzalez, C.; Challacombe, M.; Gill, P. M. W.; Johnson, B.; Chen, W.; Wong, M. W.; Andres, J. L.; Gonzalez, C.; Head-Gordon, M.; Replogle, E. S.; Pople, J. A. *Gaussian 03*, revision B03, Gaussian Inc., Pittsburgh, PA, 2003.
40. Politzer, P.; Lane, P.; Murray, J. S.; Concha, M. C. *J. Mol. Model* **2005**, *11*, 1.
41. Peralta-Inga, Z.; Lane, P.; Murray, J. S.; Boyd, S.; Grice, M. E.; O'Connor, C. J.; Politzer, P. *Nano Lett.* **2003**, *3*, 21.
42. Hoffmann, A.; Sebastiani, D.; Sugiono, E.; Yun, S.; Kim, K. S.; Spiess, H. W.; Schnell, I. *Chem. Phys. Lett.* **2004**, *11*, 164.